Technical report : Partial-wave analysis of $\bar{p}d$-annihilations into $\pi^-\pi^0\pi^0 p_{spectator}$ Evidence for ϱ'-production in $\bar{p}d$-annihilations

Christoph Straßburger

Institut für Strahlen- und Kernphysik, Rheinische Friedrich-Wilhelms Universität Bonn,
D-53115 Bonn, Germany

Abstract

This technical report presents the selection and the Partial-wave analysis of the $\pi^-\pi^0\pi^0(p_{spectator})$ final state. Data were taken from both run-periods in 1991 with LD_2 (May,October) and from June 1994. After all cuts, 123.409 $\pi^-\pi^0\pi^0$-events with $p_{spectator}$ lower than 100 MeV/c were found. A partial wave analysis was applied, yielding strong evidence for the production of two high-mass (I=1) vector-mesons.

First we consider the technical aspects of the data extraction. The following data have been used:

- minimum bias data from May,October 91 (determination of branching ratio)
- 1-prong triggered data from May 91
- 1-prong triggered data from October 91
- 1-prong triggered data from June 94

The following CBAR programs have been used:

- CBOFF 1.29/00
- GTRACK 1.35/00
- BCTRAK 2.04/00
- LOCATER 2.00/00
- CBKFIT 3.09/00
- CBGEANT 5.03/01

1 Aspects of the data-selection

The data were tracked with the Fast-Fuzzy-algorithm for the reconstruction of charged particles [1]. For the reconstruction of PED's in the barrel, the following tresholds were set : ECLUBC = EPEDBC = 20 MeV and ECLSBC = 10 MeV. In addition to the matching done by GTRACK, all clusters containing a merged ped from a charged track were dropped. These are the same cuts as applied in the analysis of branching ratios in liquid deuterium [3] and by the analysis of the ηX and η'X branching ratios [2]. Table 1 presents a detailed overview of the data-selection. Figure 1 shows the number of hits per track, as well as the first and the

Table 1: Numbers from the dataselection

	may 91	october 91	june 94
events on tape	535.091	2.476.325	5.197.960
1 long track (ge. 15 hits)	359.905	1.708.601	3.823.530
1 long,neg. track + 4 unm. peds + MM^2-cut	25.005	129.681	363.788
CL (1C-fit) $\geq$ 10%	7514	52.082	146.699
CL (3C-fit) $\geq$ 10%	7497	50.528	142.632
$p_{spectator} \leq$ 100 MeV/c	3.972	31.512	87.915

last layer distributions. In addition the missing mass squared after the preselection is shown. The cut on the missing mass squared (see figure 1 d) selects the kinematically complete events. The γ-multiplity distribution, after the cut requiring long tracks (gt 12 hits), is shown in figure 2. Kinematic fits with the values and errors extracted from the TTKS-bank show systematic deviations of the pulls. Accordingly, corrections to the TTKS-bank entries were applied, following the method

suggested by N. Djaosvili (talks presented at the meetings in October 1995 and March 1996). For the data from June 94 only a very small correction has needed to be applied. Table 2 shows the factors and Figure 3 shows the pulls from the 3C-kinematic fit. A 10% confidence level cut was applied. For the partial wave analysis

Table 2: Correction factors, used by the kinematic fit

Correction for	May91	Oct91	June94
Ψ	1.3	1.3	1.2
tanλ	1.3	1.3	1.2
$\frac{1}{p_{xy}}$	- $\frac{1}{18GeV}$	- $\frac{1}{18GeV}$	- $\frac{1}{38GeV}$

one selects the subsample with a real spectator proton. This requires a cut to be placed on the spectator-momentum at 100 MeV/c. Figure 2 b) shows the associated confidence-level distribution and figure 4 the proton-momentum distribution. Figures 5 and 6 show the $\pi^-\pi^0\pi^0$ Dalitz plot and the 1-dim. mass projections ($\pi^0\pi^0$ and $\pi^-\pi^0$). The Dalitz plot shows the pronounced structures from the two ϱ^--bands and the typical angular distribution of the $f_2(1270)$, decaying from $^1S_0$ and $^3P_1$. In the region where the two ϱ-bands are cross, a clear band from a resonance of the $\pi^0\pi^0$-system is visible. A great advantage of the $\pi^-\pi^0\pi^0$-dataset is the absence of ϱ^0-production. Without this contribution, interference of high-mass $\pi\pi$-P-wave resonances can clearly be seen on the Dalitz plot boundary. The arrows in figure 5 show the interference of the $\varrho'(1450)$. The partial wave analysis presented in this report will provide the evidence for this amplitude. The angular distribution of this ϱ' guides us to include a large contribution from $^1S_0$, because of $w(\Theta) = cos^2\Theta$. In the corner of the right side, i.e. for high masses of the $\pi^-\pi^0$-system, indications of a second high-mass $\pi\pi$-P-wave resonance can be seen. The angular distribution, although covered by the dominating ϱ^--band on one side, leads us to conclude the existence of a sizeable contribution from $^1S_0$. We have combined the data taken in 1991 and 1994 with two different JDCs, because a comparison of the data with a χ^2-test shows that the two datasets have no obvious differences ($\chi^2 = 1.14$). Figure 7 a) shows the χ^2-distribution for points with $\chi^2 \geq 4$. Accordingly, we merge the two subsamples for further partial wave analysis. The same behaviour was observed for the acceptance, as determined by MC-simulation. The acceptance is also shown in Figure 7 and the data were corrected by this acceptance before applying the partial wave analysis. For the Dalitz plot analysis, a binsize of 0.075 GeV/c^2x 0.075 GeV/c^2 was choosen. With this binsize, 825 active bins (excluding the bins which are on the edge of the Dalitz plot) were used for fitting.

1.1 Background

First, the combinatorical background from the other 1-prong 4γ channels was considered. Monte-Carlo simulations showed no contribution from $\pi^-\pi^0\eta$ and $\pi^-\eta\eta$ to the $\pi^-\pi^0\pi^0$-final state. For possible background contributions from states with unseen neutral particles like $\pi^-\pi^0\omega$, the cut on low spectator momentum provides highly efficient suppression. This is due to the fact, that most of the unmeasured momentum is caried by the proton and shifts the proton-momentum above 100 MeV/c^2 threshold . The other background source comes from $\pi^-\omega$ with one additional PED in the barrel. Of 20.000 MC-events ($\omega \rightarrow \pi^0\gamma$), only 16 events were misidentified as true $\pi^-\pi^0\pi^0$-events. The 20.000 MC-events are equivalent to

230.000 'true' $\pi^-\omega$-events, decaying via all allowed decay-chains. With the $\pi^-\omega$-branching ratio from [3] and the enhancement factor of 22.5 for the 1-prongs, $\simeq 64$ background-events are expected in the final sample. This number (0.05%) is negligible, because for such background events the $(\pi^0\pi^0)$ should peak around 780 MeV/c^2 and no indication of a stronger background contribution can be found in the final data-set. For all background studies, the hadronic package FLUKA was used. The reliability of this package, concerning the description of hadronic split-offs in the barrel, was demonstrated by the consistency of the the $\omega\ \pi^-\mathrm{p}_{spectator}$-branching ratio for the two decay-modes [3].
The only small visible contribution of background that can be seen is in the $(\pi^0\pi^0)$-mass projection. A small K^0_s-signal is visible. The small background of about 0.5% is due to the high momentum of the K^- from $\bar{\mathrm{p}}\mathrm{d} \rightarrow \mathrm{K}^-\mathrm{K}^0_s\mathrm{p}_{spectator}$. For momenta above 700 MeV/c, a pion-kaon separation is not possible with our detector. Therefore this contribution cannot be suppressed, but this small fraction is homogeniously distributed over the allowed mass region in the Dalitz plot and does not affect the physics of the $\pi^-\pi^0\pi^0$ final state.

2 Partial wave analysis

In the $\pi^-\pi^0\pi^0\mathrm{p}_{spectator}$ (for the sake of simplicity and because of the cut requiring low spectator momenta we drop $\mathrm{p}_{spectator}$) final state, resonance behaviour can be found in the $\pi^0\pi^0$-system ($\pi\pi$-S- and -D-wave) and in the $\pi^0\pi^-$-system ($\pi\pi$-P-wave). The $\pi\pi$-S- and -D-wave were precisely determined in the $3\pi^0$-system with huge statistics. Because of the additional strong contributions of the $\pi\pi$-P-wave, we fix, here, the S- and D-wave parametrizations and varied only production-strength and phase. Without the interference of two low mass $\pi\pi$-S-waves (as in the corners of the $3\pi^0$-Dalitz-plot), the $\pi^-\pi^0\pi^0$-data have a large sensitivity to the high mass $\pi\pi$-D-wave resonance, i.e. this data can test the presence of the $f_2(1540)$, as claimed by several data analyses [6, 7, 8]. Moreover, a free fit to determine mass and width of the $f_2(1540)$ was done and we comment on the result later. The dynamical amplitude is described with the well-known K-matrix formalism, an extended review of which can be found in [11]. For the $\pi\pi$-P-wave one can choose a 1x1-K-matrix, because the the $\varrho(770)$ is totally elastic and the large number of possible decay-chains of the high mass vector-mesons do not support an introduction of one additional decay-channel with a 2x2-K-matrix. The introduction of a second, unmeasured partial width would introduce correlated parameters, which one should avoid (see [11]). The 1x1-K-matrix guarantees a unitary description in the case of the overlapping high-mass resonances. The angular distributions were calculated within the standard Zemach-formalism.

2.1 Description of the fits

A first fit was made with the solutions for the $\pi\pi$-S- and -D-wave from the 4-pole solution of [8]. To mention the poles explicitly (T-matrix poles) : $f_0(980)$, $f_0(1100)$, $f_0(1370)$, $f_0(1500)$, $f_2(1275)$ and $f_2(1540)$. For the $\pi\pi$-P-wave only the well known $\varrho(770)$ was introduced. The fit resulted in a bad χ^2 of 6522; illustrated by figure 9,, which shows clear deviations from the data in the region where the high mass ϱ's are expected (fit 1, table 4). For the next fit, the two further $\pi\pi$-P-wave resonances were introduced. Masses and widths were taken from the result of Donnachie and Clegg [4]. The χ^2 improves extremely. With the fixed masses and widths of the additional ϱ''s (only the $\varrho(770)$ was varied freely) the fit ends at a χ^2 of 1330 (fit 2). In the next step, the masses

and widths of the ϱ''s were varied in addition. χ^2 improves slightly to 1300 at a stable minimum with excellent convergence (fit 3). Figure 8 shows the agreement of data and fit result for the two mass-projections. In addition, the $+\chi^2$- and -χ^2 distributions are shown. Large χ^2-differences only arise in individual, isolated cells, contributing more than 4 to the overall χ^2. For many reasons which will be discussed in what follows, this fit represents the preferred solution. For the parameters of the $\pi\pi$-P-wave a full MINOS analysis was performed and table 3 illustrates results of the error-analysis.

Table 3: Masses and widths of $I = 1$-vectormesons

M_ϱ	=	763.7 ± 3.1	Γ_ϱ	=	152.8 ± 4.2
M_ϱ	=	1411 ± 10	Γ_ϱ	=	343 ± 18
M_ϱ	=	1780^{+34}_{-25}	Γ_ϱ	=	275 ± 42

A first check drops the second high-mass vector-meson, which is still found at the end of phase-space. The $\pi\pi$-P-wave with two poles was then varied freely. The resulting χ^2 was worse by 144 units and the ϱ' was shifted down in mass to 1387 MeV/c^2 with a width of 564 MeV/c^2. Figure 10 shows the mass-projections and the χ^2-distributions. From the mass-projections themselves, no obvious difference from the 'bestfit' can be seen. On the other hand the χ^2-plots show, exactly at the band structure a slightly worse description. One can interpret this fit result as a further indication of the presence of a second ϱ', but the large errors of mass and width from the MINOS-analysis demonstrate the limited sensitivity of the data in a precise determination of the resonance parameters. In [8] two solutions of the $\pi\pi$-S-wave were shown. In the first fits, the 4-pole solution was choosen. Taking the 3-pole solution (without the relatively narrow $f_0(1370)$, but still including the two D-wave poles), the χ^2 improves by 63 units, but with worse convergence for the $\pi\pi$-P-wave. Moreover, the ϱ' was shifted down in mass to 1182 MeV/$c^2$and the width broadened to 470 MeV/c^2. Although χ^2 is improved by 63 units, one shoud not consider this solution take the best one, because of the worse convergence. Figure 12 shows the interference-structures for a 'narrow' ϱ' at 1420 MeV/$c^2$and for a broad ϱ' at 1200 MeV/c^2. There is only a small difference for the ϱ'interference-region, but a major difference (see $^1S_0$!) for the region where $f_0(1100)$, $f_0(1370)$, $f_0(1500)$, $f_2(1270)$ and $f_2(1540)$ interfere. The coupled channel analysis of the 3 pseudoscalar final states with neutral particles is much more sensitive to this region. Therefore, the consistency of the 4-pole $\pi\pi$-S-wave in our coupled channel analysis [10, 9] and the excellent convergence of the $\pi\pi$-P-wave with the 4-pole-S-wave parametrization underlines the evidence, that the fit with the 3-pole-S-wave parametrization is not the favoured solution.
Recently, the LASS experiment [13] reported evidence for a low–mass (1287$\pm$14 MeV) ϱ' in the analysis of data on $K^- \rightarrow \Lambda\ \pi^+\pi^-$. This value is in accordance with the value expected from the mass of the $K^*(1410)$. The fit number 3 was tried with different start-parameters, especially with the narrow ϱ' at 1300 MeV/c^2. In all cases, the solution 3 was reproduced. This rules out the possibility of a narrow $\varrho'(1300)$ instead of the one at 1420 MeV/c^2. A simulation of the interference-region of a possible narrow $\varrho'(1300)$ shows immediately without any fit, that our data does not accomodate a narrow $\varrho'(1300)$ (figure 11). A narrow $\varrho'(1300)$ would produce a blob-like interference-pattern, different from our observed band-structure. But there could

Table 4: Compilation of fit results

Fit	$\pi\pi$-S-wave	$\pi\pi$-P-wave	$\pi\pi$-D-wave	$^1S_0$	$^3P_1$	$^3P_2$	χ^2
1	$f_0(980), f_0(1100)$ $f_0(1370), f_0(1500)$	$\varrho(770)$	$f_2(1275)$ $f_2(1540)$	35.3%	40.6%	24.1%	6522
2	$f_0(980), f_0(1100)$ $f_0(1370), f_0(1500)$	$\varrho(770),\ \varrho^+(1450)$ $\varrho^+(1700)$	$f_2(1275)$ $f_2(1540)$	47.3%	33.8%	18.9%	1330
3	$f_0(980), f_0(1100)$ $f_0(1370), f_0(1500)$	$\varrho(770),\ \varrho^+(1450)$ $\varrho^+(1700)$	$f_2(1275)$ $f_2(1540)$	51.4%	29.1%	19.6%	1300
4	$f_0(980), f_0(1100)$ $f_0(1370), f_0(1500)$	$\varrho(770),\ \varrho^+(1450)$	$f_2(1275)$ $f_2(1540)$	44.4%	41.4%	14.2%	1447
5	$f_0(980), f_0(1100)$ $f_0(1500)$	$\varrho(770),\ \varrho^+(1450)$ $\varrho^+(1700)$	$f_2(1275)$ $f_2(1540)$	46.7%	29.6%	23.7%	1237
6	$f_0(980), f_0(1100)$ $f_0(1370), f_0(1500)$	$\varrho(770),\ \varrho^+(1450)$ $\varrho^+(1700)$	$f_2(1275)$	47.4%	28.5%	24.1%	1510
7	$f_0(980), f_0(1100)$ $f_0(1370), f_0(1500)$	$\varrho(770),\ \varrho^+(1300)$ $\varrho^+(1450)\ \varrho^+(1700)$	$f_2(1275)$ $f_2(1540)$	50.4%	28.5%	21.1%	1212

be in addition a ϱ' at 1300 MeV/c^2, because the nature of the $\varrho'(1450)$ is still controversial [14]. A fit with 4 free $\pi\pi$-P-wave poles was tried. The fit resulted in a χ^2 improved by 88 units and the 4 poles were found at 763.5-i77, 1321-i92, 1368-i128 and 1807-i139. It is likely, that only the additional flexibility is responsible for the improvement in χ^2 – one should not claim the observation of four isovector vector resonances.

In addition to the observation of high-mass P-wave-resonances, the $\pi^-\pi^0\pi^0$-data can verify the existence of the $f_2(1540)$. In contrast to the $3\pi^0$-final state, the $\pi\pi$-D-wave does not interfere with the low mass $\pi\pi$-S-wave. Only interferences with the ϱ^- are present, and the ϱ^--parameters are much better known than the $\pi\pi$-S-wave parametrization. This is demonstrated by the ϱ^- values resulting from the MINOS-analysis 3, which are in perfect agreement with those given by the Particle Data Group [5]. For the next fit, where the $f_2(1540)$ was dropped, the χ^2 was worse by 210. A fit with free mass and width for the $f_2(1540)$ yields the following result (MINOS-analysis of the errors):

$$f_2(1540): \quad \mathrm{m}=(1514 \pm 3.4)\,\mathrm{MeV}/c^2 \quad \Gamma=(145 \pm 6)\ \mathrm{MeV}/c^2$$

The χ^2 of the free fit improves by 20 units. This fit is not a precise determination of mass and width, because the mass and width of the $f_2(1540)$ is strongly influenced by the parametrization of the $f_0(1500)$. The present data-set is not adequate to fit with S- and D-wave free. Only a combined fit with the 3 π^0 is able to shed more light to the $f_2(1540)$ parameters. This will be one goal in a combined fit of all 3 π data-sets. This improvement in χ^2 on adding the $f_2(1540)$ here is significant enough to establish once more the presence of this tensor-state. Table 4 is the summary of all fits described until now.

To determine the branching fractions of the individual $\pi\pi$-P-wave contributions,

all parameters (masses, widths,production-strengths and phases) of $\pi\pi$-S- and $\pi\pi$-D-wave were fixed. The K-matrix parametrization was replaced by 3 relativistic Breit-Wigners and only the P-wave was fitted free. The contributions of the initial states are : $^1S_0$: 49%, $^3P_1$: 26% and $^3P_2$: 25%. The errors are dominated by systematic uncerntainties and are of the order $\pm$ 2%. The contributions of the vector-mesons to the total intensity of the Daltiz plot are given in table 5. The errors

Table 5: Branching fractions of the vectormesons

initial state	$\varrho(770)$	$\varrho(1450)$	$\varrho(1700)$
$^1S_0$	8.2%	9.6%	3.0%
$^3P_1$	6.2%	3.3%	1.0%
$^3P_2$	4.3%	2.6%	5.9%

of the individual contributions are still dominated by systematic effects (Breit-Wigner instead of K-matrix parametrization) and are about 1-2% (for example 8.2$\pm$1-2%).

2.2 Coupled fit with $\pi^+\pi^-\pi^0$

A last test was done with a coupled fit to $\pi^-\pi^0\pi^0$ and $\pi^+\pi^-\pi^0$. For the $\pi^+\pi^-\pi^0$ Dalitz plot, all 2-prong-triggered data from 1991 were used. Tracks and PEDs were selected with the definitions given by the CERN-Tracking-Group [12]. A 5C-fit to the hypothesis $\pi^+\pi^-\pi^0$ was performed with a confidence-level cut of 10%. Anti-cuts to other possible 2-prong plus two γ-hypothesis were done. Furthermore, Monte-Carlo simulations showed that the selected sample of 181,000 events is free from any type of background. $^1S_0$, $^3P_1$ and $^3P_2$ initial states are included for both data-sets, whereas in the $\pi^+\pi^-\pi^0$-final state $^3S_1$ and $^1P_1$ are allowed in addition. For the annihilation from the common initial states the amplitudes were coupled by requiring isospin-invariance. Explicitly taken into account was the factor 2 reduction of the amplitude in the $\pi^0\pi^0$-system (two identical particles, $\pi\pi$-S- and -D-wave).

$$\begin{aligned}
\pi\pi\text{-P-wave} &: A_{\pi^\pm\pi^0} = \mathrm{a} \cdot A_{\pi^-\pi^0} \\
\pi\pi\text{-S-wave} &: A_{\pi^+\pi^-} = \mathrm{a} \cdot \sqrt{2} \cdot A_{\pi^0\pi^0} \\
\pi\pi\text{-D-wave} &: A_{\pi^+\pi^-} = \mathrm{a} \cdot \sqrt{2} \cdot A_{\pi^0\pi^0}
\end{aligned}$$

The fit converged properly with a χ^2 of 1338 for $\pi^-\pi^0\pi^0$ and 1273 for $\pi^+\pi^-\pi^0$. Both Dalitz plots have 825 active cells for fitting. Table 6 summarizes the contribution of each initial state. The total amount of P-wave of 16.8% in $\pi^+\pi^-\pi^0$ is in good

Table 6: Contribution of the initial states, Isospin-invariant fit

final state	$^1S_0$	$^3S_1$	$^1P_1$	$^3P_1$	$^3P_2$
$\pi^-\pi^0\pi^0$	48.1%	–	–	34.3%	17.6%
$\pi^+\pi^-\pi^0$	9.2%	74.0%	6.5%	4.8%	5.5%

agreement with the expectation of about 13%. This demonstrates, that a large P-wave fraction in deuterium is still compatible with our overall value of initial P-wave annihilation in liquid hydrogen.

3 Summary

The selection and the partial wave analysis of the reaction $\bar{p}d \to \pi^-\pi^0\pi^0 p_{spectator}$ has been presented. For the partial wave analysis, the subsample of events with $p_{spectator}$ lower than 100 MeV/c was used, in order to allow for annihilations on the free neutron. For the $\pi\pi$-S- and $\pi\pi$-D-wave the pole-structures from the high statistics $3\pi^0$-analysis and the coupled channel analysis were used. The $\pi\pi$-P-wave was fitted freely and evidence for 2 high-mass vector-mesons was found. The parameters of the $\pi\pi$-P-wave are given in table 3. The presence of the $f_2(1540)$ is seen in this analysis to be required. A fit without this tensor was worse by 212 units in χ^2.

References

[1] M. Benayoun et. al.,Fast Pattern Recognition with JDC data based on Fuzzy-Radon transform properties, CB-Note 276

[2] F.-H. Heinsius, Eta-Decays into 3 Pions, Technical report CB-Note 231

[3] C. Straßburger, Determination of branching ratios in liquid deuterium, CB-Note 254/1, in preparation (see talk at meeting in january 1996)

[4] A.Donnachie & A.Clegg, Zeitschrift f. Physik **C62** (1994) 455

[5] Particle Data Group (PDG), Phys. Rev. **D50** (1994) 1479

[6] B. May et. al., Zeitschrift f. Physik **C46** (1990) 203

[7] Adamo et. al., Nucl. Phys. **A558** (1993) 13C

[8] Crystal Barrel Collaboration, C. Amsler et. al., Phys. Lett. **B342** (1995) 433

[9] Crystal Barrel Collaboration, A. Anisovich et al., Phys. Lett. **B323** (1994) 233

[10] Crystal Barrel Collaboration, C. Amsler et al., Phys. Lett. **B355** (1995) 425

[11] S.U.Chung et al., Ann. d. Physik **4** (1995) 404

[12] M.Benayoun,N. Djaoshvili,C. Völcker et. al., JDC data errors, CB-Note 295

[13] D. Aston et. al., Talk presented at Hadron93, Como,Italy

[14] F. Close, P. Page, The production and decay of hybrid mesons by flux tube breaking, RAL-94-116

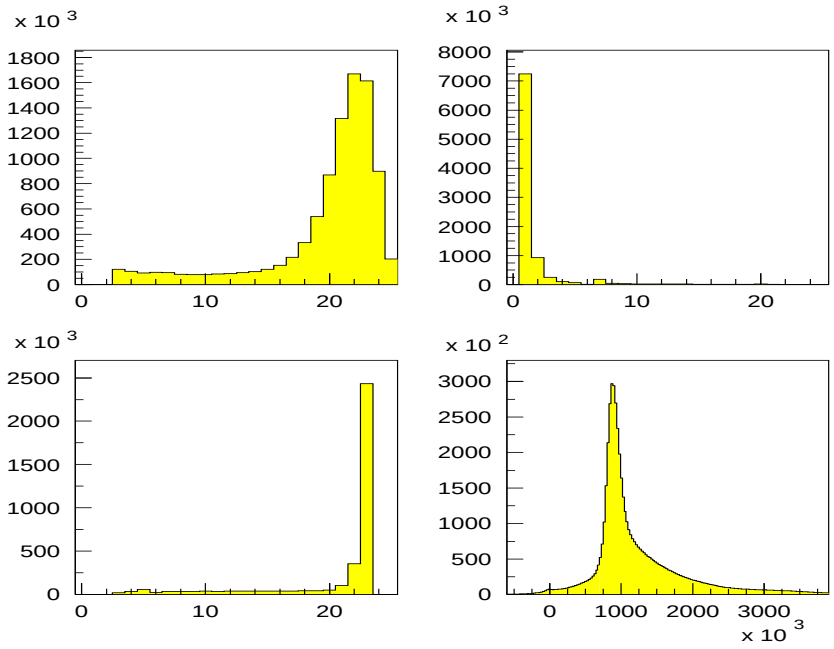

Figure 1: a) Number of hits per track, b) first layer, c) last layer and d) missing mass square

4 Figures

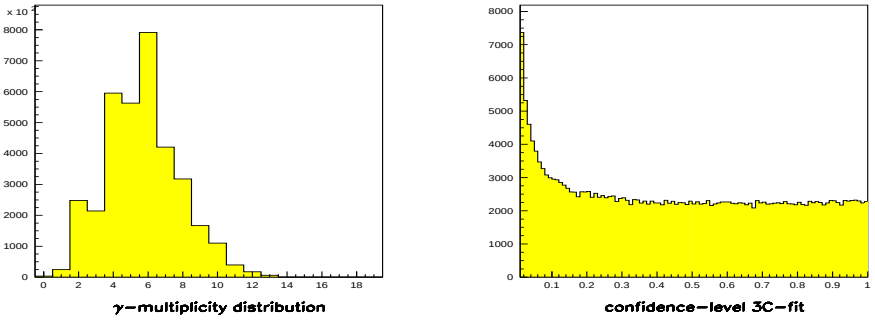

Figure 2: γ-multiplicity distribution and confidence-level of 3C-fit

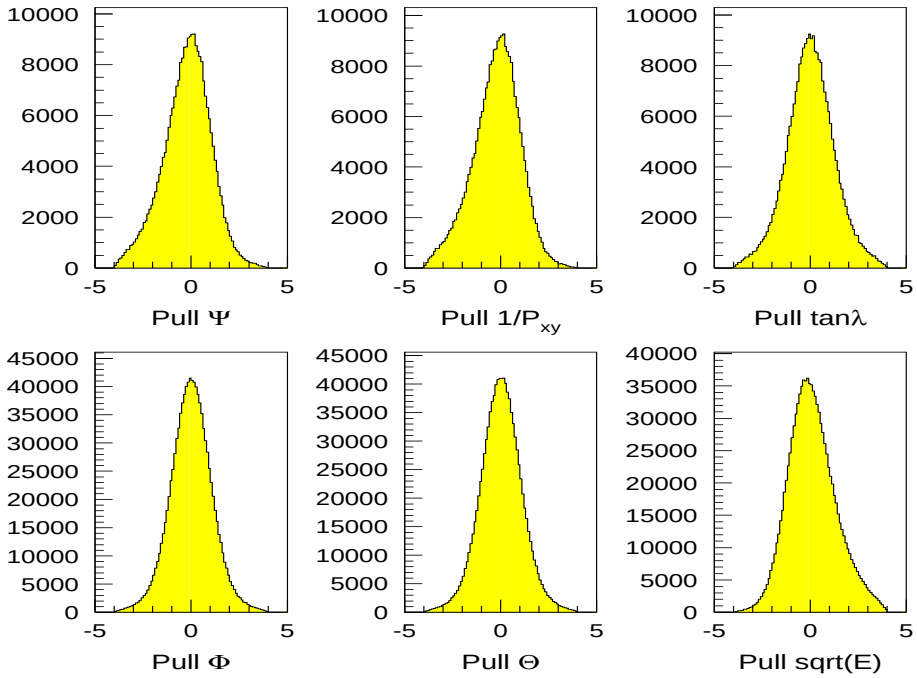

Figure 3: Pulls of the 3C-kinematic fit

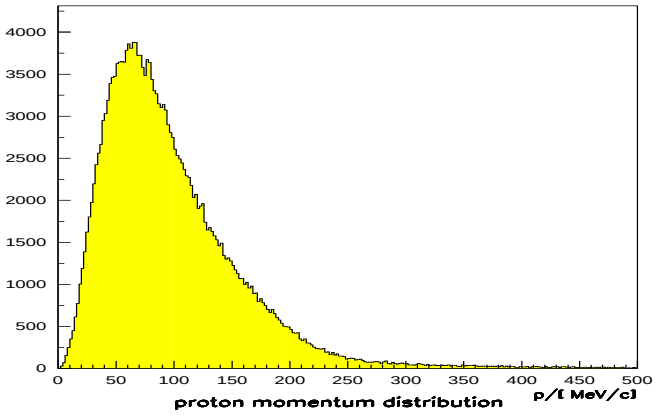

Figure 4: Distribution of the proton-momentum from the 3C-fit

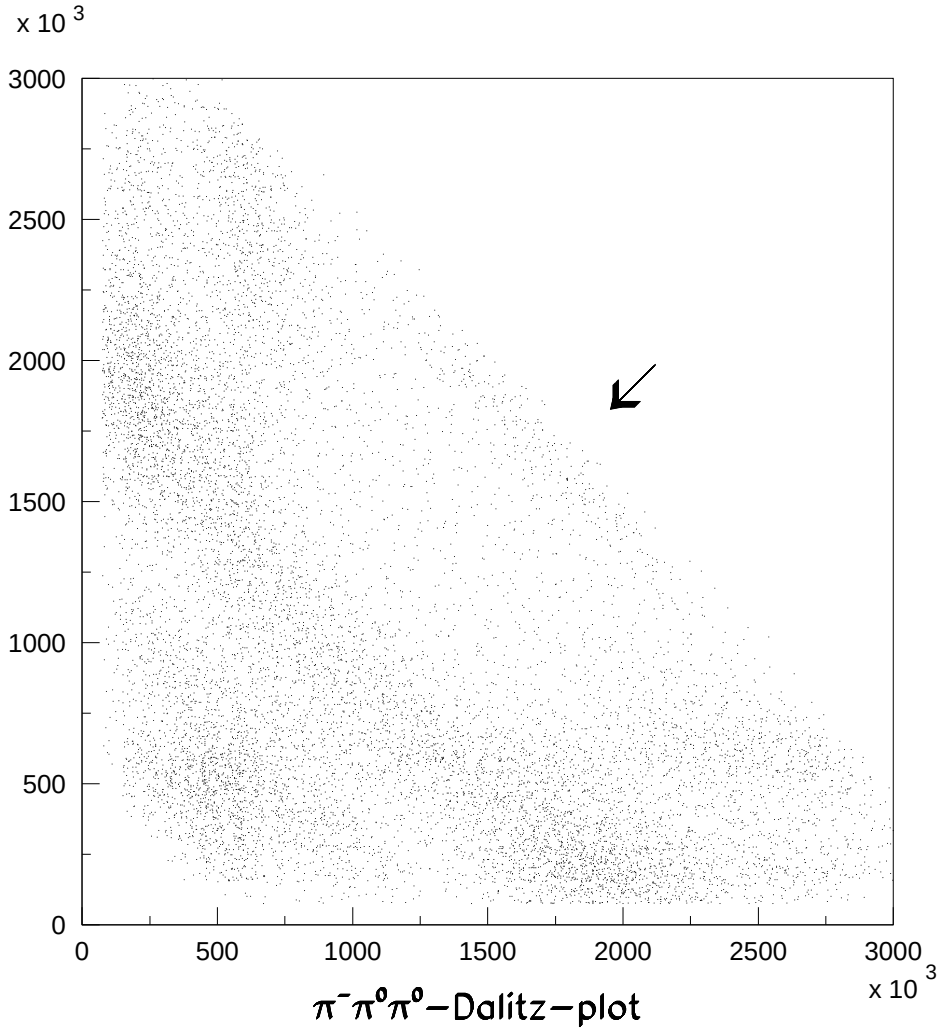

Figure 5: $\pi^-\pi^0\pi^0$Dalitz-plot ($p_{spectator} \leq 100$ MeV/c)

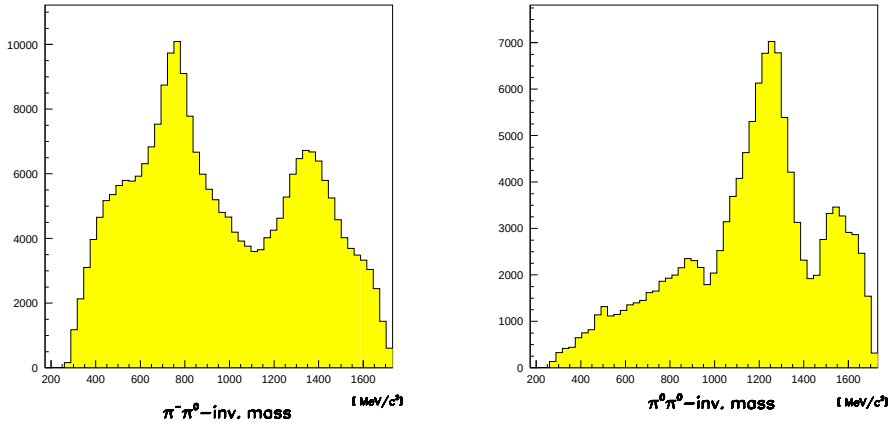

Figure 6: a) $\pi^-\pi^0$ invariant mass, b) $\pi^0\pi^0$ invariant mass

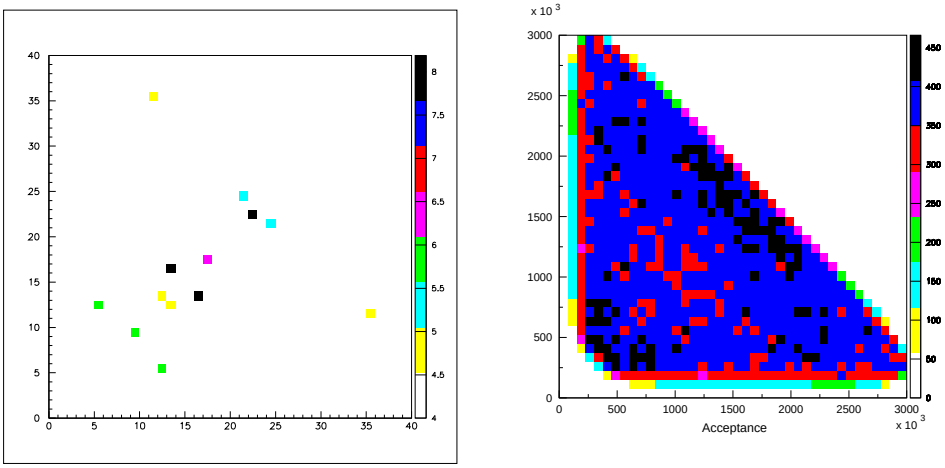

Figure 7: comparison of 91- and 94-data and acceptance

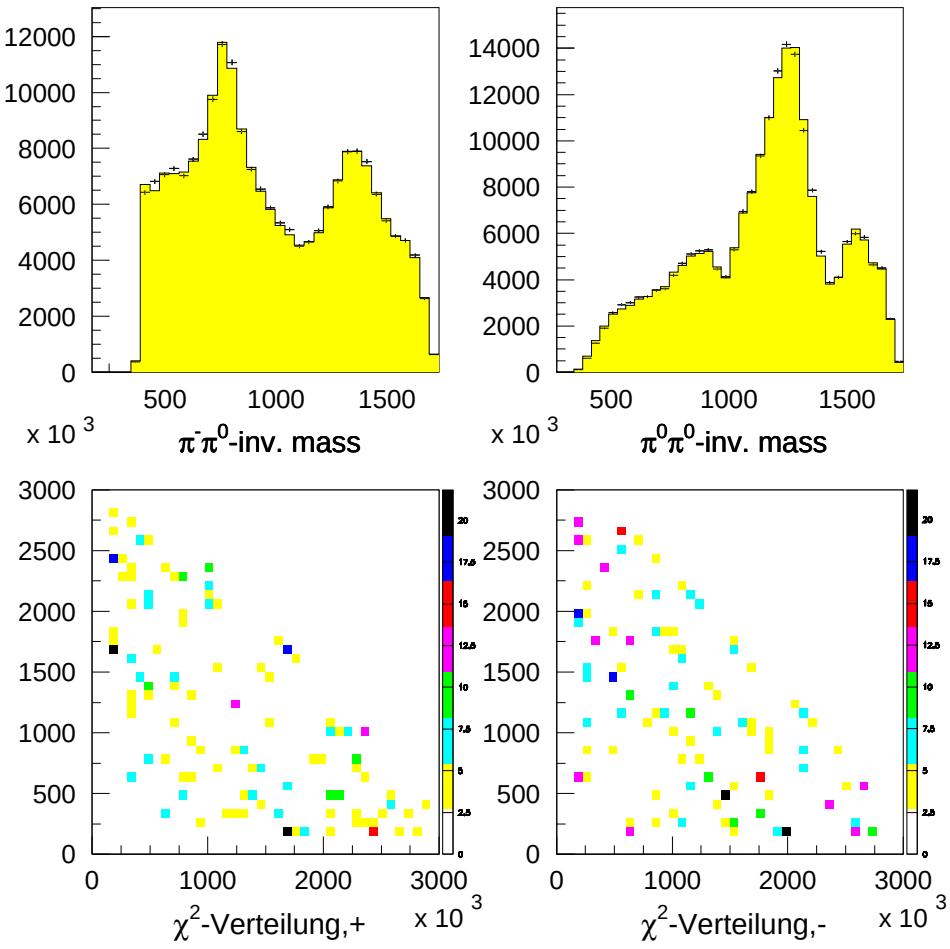

Figure 8: Fit Number 3, best fit to the data

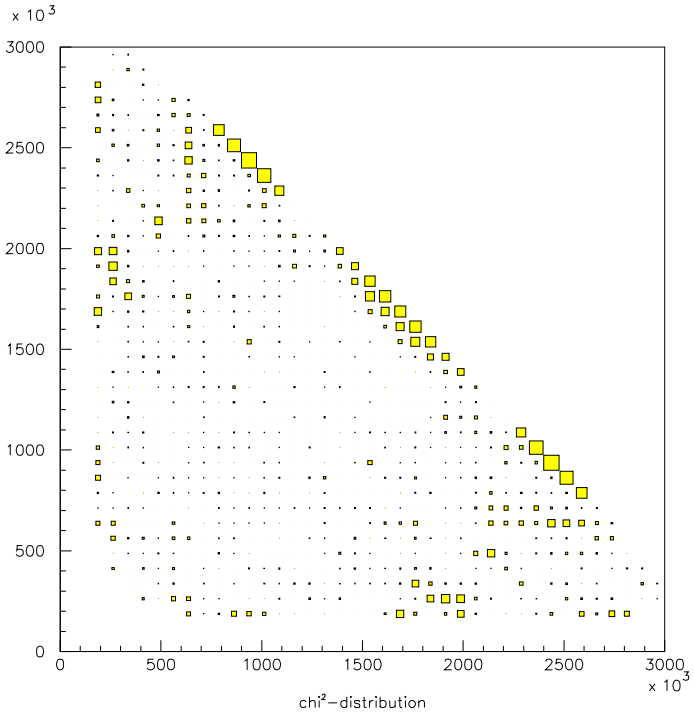

Figure 9: χ^2-distribution of the fit with only $\varrho(770)$ in the $\pi\pi$-P-wave

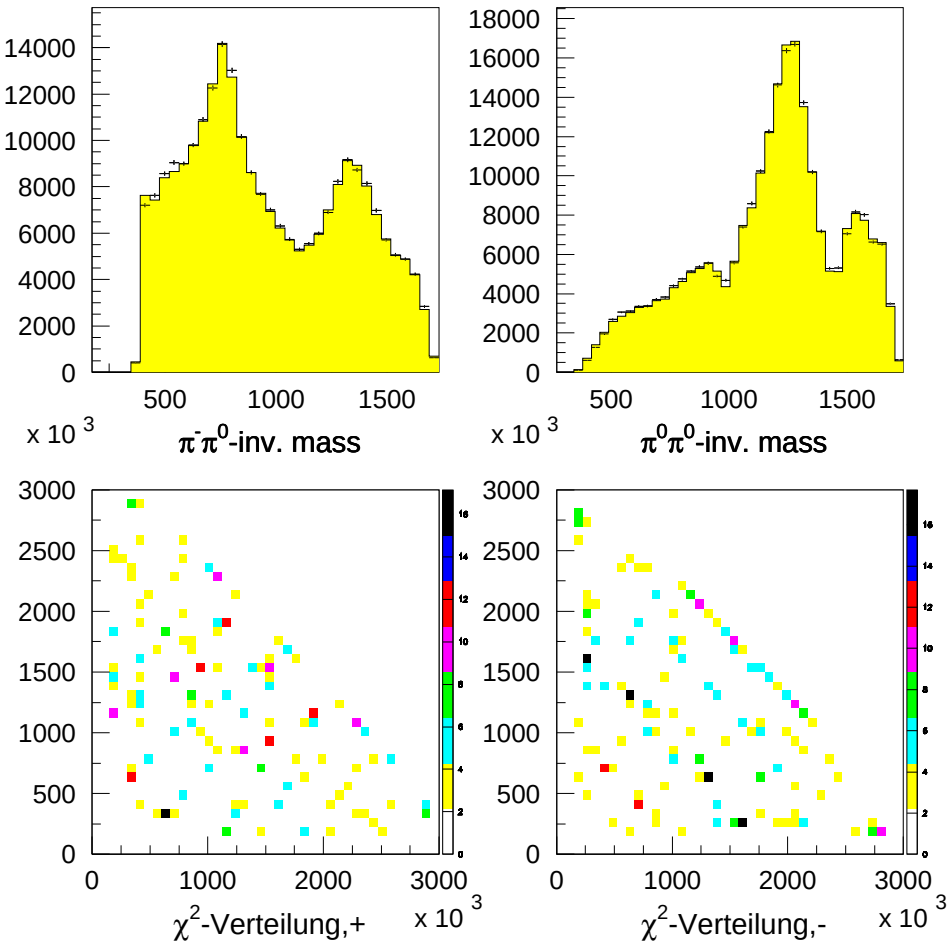

Figure 10: Fit with two resonances of the $\pi\pi$-P-wave

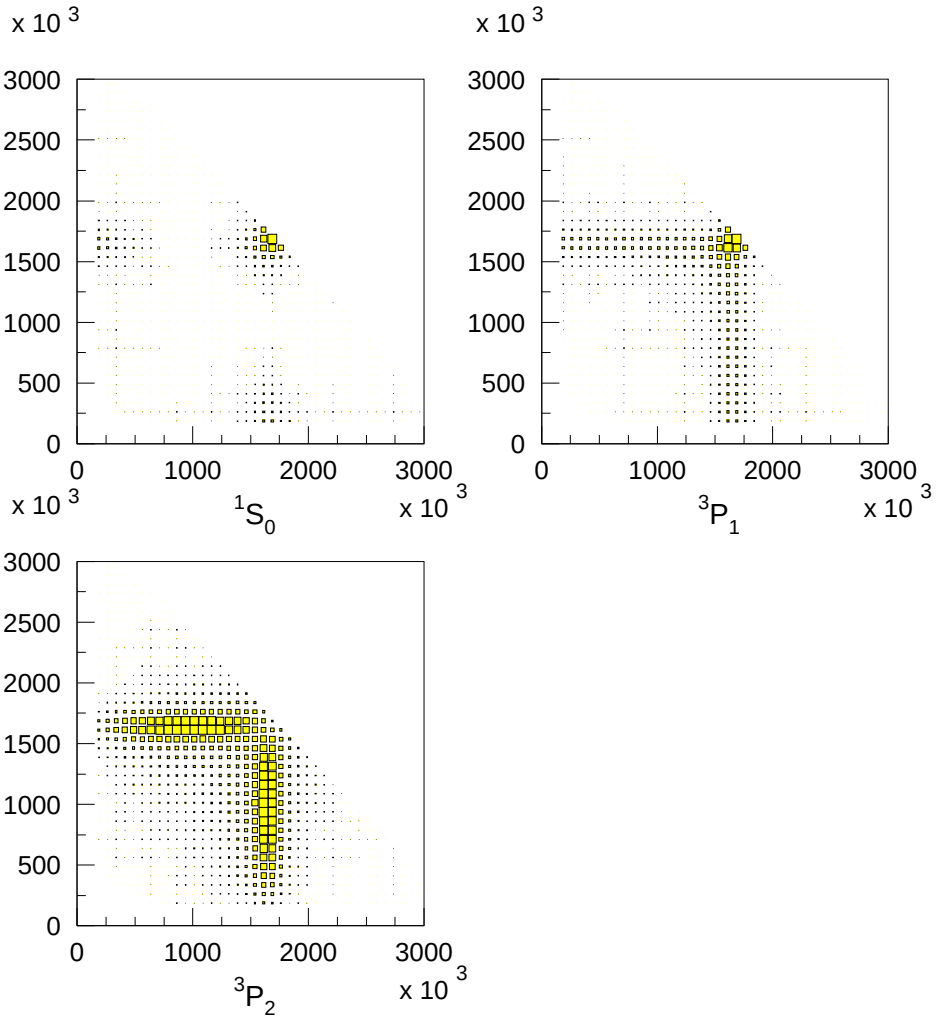

Figure 11: Simulation of a narrow $\varrho(1300)$ from the a)$^1S_0$ b)$^3P_1$ and c)$^3P_2$-initial states

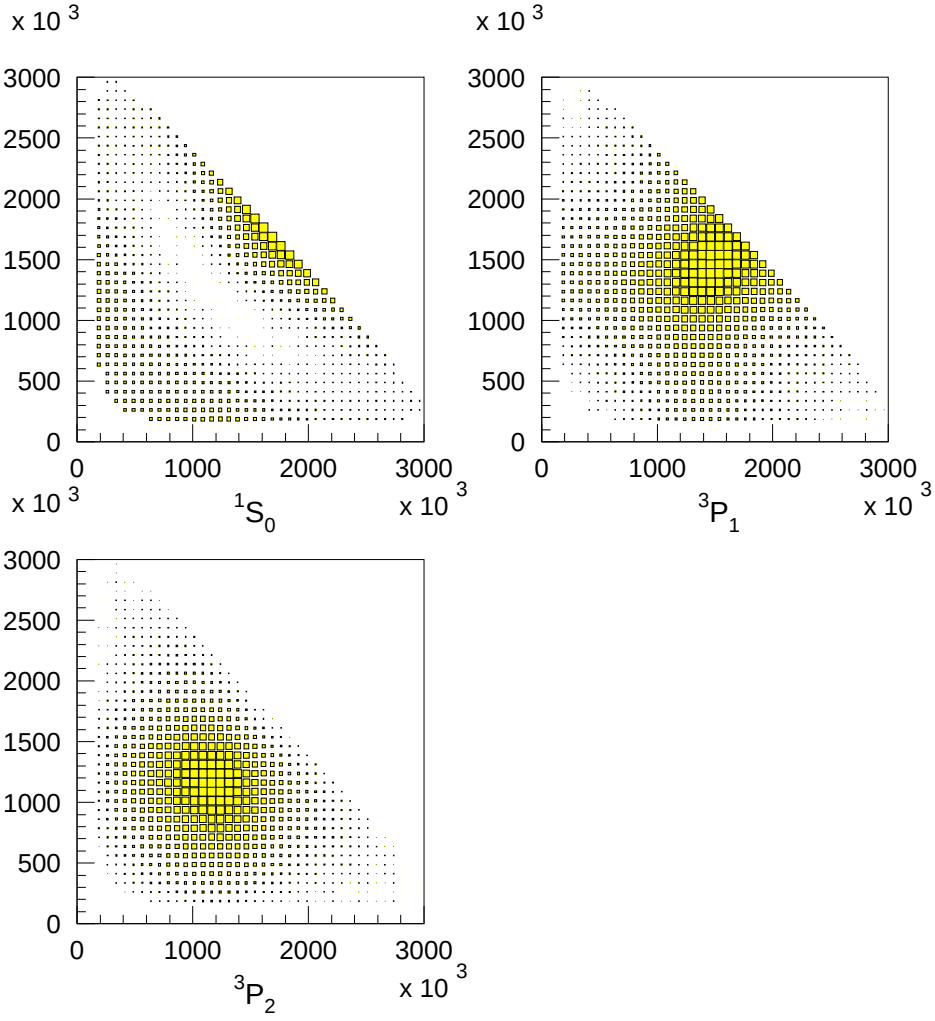

Figure 12: Simulation of a $\varrho(1200), \Gamma = 500$ from the a)$^1S_0$ b)$^3P_1$ and c)$^3P_2$-initial states

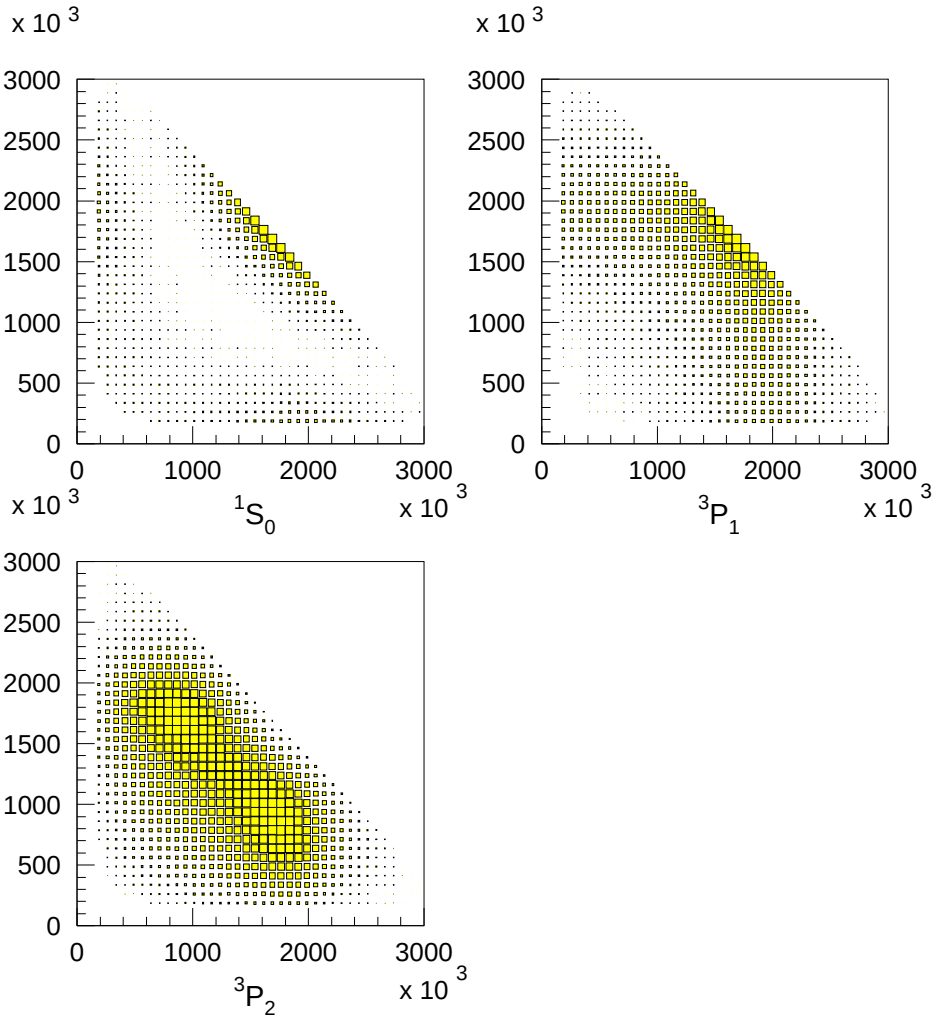

Figure 13: Simulation of a $\varrho(1420)$, $\Gamma = 320$ from the a)$^1S_0$ b)$^3P_1$ and c)$^3P_2$-initial states